J. exp. Biol. **107**, 431–449 (1983)
Printed in Great Britain © *The Company of Biologists Limited 1983*

GRADED POTENTIALS AND SPIKING IN SINGLE UNITS OF THE OVAL ORGAN, A MECHANORECEPTOR IN THE LOBSTER VENTILATORY SYSTEM

I. CHARACTERISTICS OF DUAL AFFERENT SIGNALLING

BY V. M. PASZTOR

Department of Biology, McGill University, 1205 Avenue Dr. Penfield, Montreal, Canada H3A 1B1

AND B. M. H. BUSH

Department of Physiology, University of Bristol, Park Row, Bristol BS1 5LS

(*Received 14 March 1983–Accepted 24 June 1983*)

SUMMARY

1. The lobster oval organ sends three afferent fibres to the suboesophageal ganglion: X (mean diameter 41 μm), Y (32 μm) and Z (22 μm). The distance between the oval organ and the ganglion is 10–15 mm in animals of approximately 10 cm carapace length.

2. The cell bodies of the sensory units lie centrally amidst the ventilatory motoneurones, and their central branches permeate the same lateral neuropile.

3. Intracellular recordings from each fibre show that the afferent response to stretch has two components: overshooting, regenerative, TTX-sensitive impulses, and an underlying graded depolarization.

4. The analogue signal has the characteristics of a receptor potential: a dynamic response with rapidly depolarizing initial component, some adaptive fall leading to a maintained static plateau, and a post-release hyperpolarizing undershoot.

5. The two signals are not equally represented in the response of the three afferents. Fibre X has the largest graded potentials (up to 30 mV in recordings 6 mm proximal to the confluence of the sensory dendrites). Fibre Z attains the highest firing frequencies (usually around 100 s^{-1}). Fibre Y has intermediate properties.

6. Both the amplitude of the graded potential and the number of spikes per response (in fibres Y and Z) relate linearly to pull amplitude.

7. Estimates of length constant (approximately 10 mm) and specific membrane resistance (100 $k\Omega cm^2$) are consistent with the hypothesis that the graded potentials spread into the presynaptic terminals with sufficient magnitude to bring about postsynaptic events.

INTRODUCTION

A search for mechanoreceptors in the ventilatory appendage of decapod Crustacea, the second maxilla, that could provide sensory feedback to the respiratory pattern

Key words: Mechanoreceptor, afferent signalling, graded potentials, Crustacea.

generator, has revealed only one proprioceptor (Pasztor, 1969). This was named the oval organ due to the oval mass of dendritic endings seen after methylene blue staining. Its support of connective tissue spans moving parts near the anterior pivot of the scaphognathite blade, and the receptor is well placed to monitor the activity of the ventilatory pump.

When compared with other crustacean proprioceptors, the oval organ presents several unusual features (Pasztor, 1979), and it cannot easily be classified into any of the well-established categories (Bush & Laverack, 1982). For example, naked bulbous terminals, instead of ciliary endings protected by scolopidia, distinguish it from chordotonal organs, and the lack of a muscle component, by definition, separates it from muscle receptor organs. Yet, the limited number of sensory neurones, their large diameter afferent fibres, and the central location of the cell bodies suggest affinities with the coxal receptor organs at the base of the walking legs, the T-C MRO and certain 'innervated elastic strands' (Alexandrowicz & Whitear, 1957; Whitear, 1965; Bush, 1976).

Ripley, Bush & Roberts (1968) first demonstrated that the T-C MRO represented a novel class of mechanoreceptors which transmitted afferent sensory information by means of graded potentials rather than frequency coded impulses. Since then, other non-impulsive mechanoreceptors have been found in the uropods of swimming crabs (Paul, 1972), and in the swimmerets of crayfish (Heitler, 1982). The anatomical similarities between the oval organ and these non-impulsive afferents, as well as the suitability of the oval organ preparation for intracellular study, prompted an investigation of sensory signalling in the oval organ. In this paper we present evidence to show that, as with the T-C MRO, graded potentials pass along oval organ afferents towards the ganglion but that, in addition, the afferents also support regenerative impulses. The possibility exists that both the analogue signal and frequency coded spikes mediate information transfer. A short report of some of these findings has already been presented (Pasztor & Bush, 1982).

MATERIALS AND METHODS

The European lobster, *Homarus gammarus*, was used for most of these experiments. Small male or female specimens (carapace length 8–10 cm) were supplied by the Marine Biological Laboratory, Plymouth, and were kept in aquarium tanks of recirculating, aerated, filtered artificial sea water at 10–15 °C.

The ventral half of the cephalo-thorax was cut out and washed thoroughly in cold running saline before being pinned, ventral side up, in a large Sylgard-lined bath for further dissection. First, the sternites and part of the endophragmal skeleton were cut away to expose the suboesophageal ganglion and the nerve trunks running to the second maxilla. Then the arthrodial membrane covering the ventral surface of the articular cavity was stripped off, revealing the maxillary musculature. Each muscle was carefully removed leaving as much of the innervation as possible *in situ*. Finally, the oval organ was exposed and isolated, leaving only the skeletal and cuticular elements attached that were needed for its support. The receptor, the connecting nerve and the suboesophageal ganglion were transferred to a smaller preparation dish.

The receptor was orientated so that the oval of cuticle at the base of the organ could

be pinned to the Sylgard lining of the dish, while the apex of the organ pointed upwards, and was pierced by the hook of the puller assembly. The nerve trunk bearing the oval organ afferents was supported by a sculpted Sylgard platform, desheathed and pinned out securely with cactus spines. Careful visual inspection throughout ensured that the organ could be exposed to a variety of mechanical stimuli without causing movement of the afferents at the intended recording locus. Superfusion with cold, aerated saline kept this preparation viable for periods of up to 10 h (507 mM-NaCl, 8·4 mM-KCl, 15 mM-$CaCl_2$, 7·5 mM-$MgCl_2$, 10 mM-Tris, 5 mM-maleic acid; pH 7·4).

Controlled stretches of the oval organ were provided by a loudspeaker-driven puller similar to that described by Bush, Godden & Macdonald (1975). For the experiments described in this study, we used single trapezoidal pulls delivered at 1-min intervals. The function generator provided variable and independent control of ramp slope, pull amplitude and plateau duration. A displacement transducer coupled to the shaft of the puller provided a linear monitor of actual hook movements. The position of the puller (and thus the length of the oval organ strands) was carefully adjusted to ensure immediate onset of depolarization at the start of stretch stimuli.

Intracellular recordings were made with 3 M-KCl-filled glass micropipettes (15–25 MΩ) inserted into the afferent fibres. Usually data were collected from two recording sites concurrently, either from two penetrations of a single afferent or, for comparative purposes, from two different fibres. D.c. recordings were led to a tape recorder, Brush recorder and CRO, and filmed from the CRO screen. Tape recordings were analysed using an Apple microprocessor and Isaac interface.

Either the central pathways or the peripheral dendrites of oval organ afferents were stained with the intensified cobalt method of Bacon & Altman (1977). Backfilling of the central or peripheral nerve stumps proceeded for 18 h at 4 °C.

RESULTS

Anatomy

The receptor consists of a cone-shaped array of individual connective tissue strands which supports the dendritic arbors of three sensory units. The cone has an elliptical base, whose longer diameter is 1·5 mm, and is 2·0 mm high. There are more than 250 separate collagenous strands arising from an oval patch of tall columnar epithelium, and inserting onto an invaginating sclerite associated with the base of the second endite (Fig. 1). *In situ* the cone is orientated vertically, with the apex pointing ventrally, and spans a narrow gap between endite skeleton and the arthrodial membrane associated with the dorsal coxo-thoracic articulation.

The nerve trunk, which carries the major sensory and motor innervation of the scaphognathite blade, runs right through the cone of connective tissue strands, but the three oval organ fibres exit, and arborize throughout the array. A dendritic branch courses alongside each connective tissue strand without further branching, until it reaches the transitional region between the strands and the epidermis. Here it proliferates further and fine, naked twigs run through the extensive basement membrane, between the basal processes of the tall columnar epidermal cells, to end in bulbous terminals anchored between the cells (Pasztor, 1979).

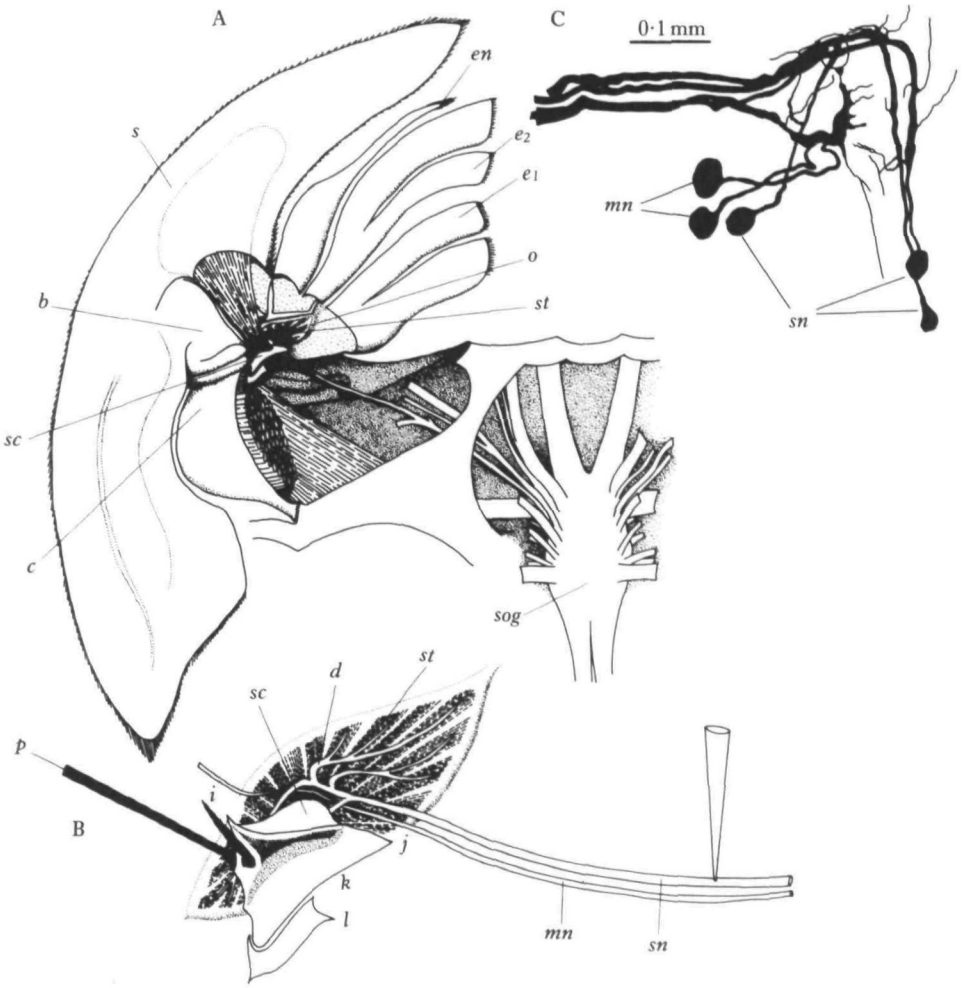

Fig. 1. (A) Diagram of partially dissected second maxilla showing the position of the oval organ. Ventral view. (B) Detail of the isolated oval organ showing the orientation of the preparation used for recording. The puller hook is inserted through the remnant of endite sclerite whose invagination provides anchorage for the array of receptor strands. Only one sensory afferent and one motor axon are shown. (C) *Camera lucida* drawing of sensory and motoneurones backfilled with cobalt through the cut scaphognathite nerve. Lateral view. Abbreviations: *b*, basipodite; *c*, coxopodite; *d*, dendrite; e_1 and e_2, first and second endites; *en* endopodite; *i–j*, cut edge of second endite sclerite; *k–l*, cut edge of first endite sclerite; *mn*, motoneurone; *o*, oval organ; *p*, puller; *s*, scaphognathite; *sc*, remnant of sclerite; *sn*, sensory neurone; *sog*, sub-oesophageal ganglion; *st*, connective tissue strands.

When the nerve trunk is desheathed, three afferent fibres can be recognized, and they are assigned names X, Y and Z in descending order of diameter. All are larger than two motor axons in the same nerve, which continue on through the oval organ to a muscle intrinsic within the scaphognathite. Mean diameters are: X, 41 μm; Y, 32 μm; Z, 22 μm. The nerve trunk from oval organ to ganglion measures 12–15 mm.

Cobalt backfilling through the cut central end of this nerve reveals that the sensory neurone somata lie within the sub-oesophageal ganglion amidst the cluster of

motoneurones supplying the appendage. Fig. 1C shows a *camera lucida* drawing of a cobalt stained preparation of the three oval organ neurones and the two motoneurones which share the same trunk. From this, and other similar preparations, it can be seen that the sensory units share the same restricted lateral neuropile as the motoneurones. Their closely interlacing branches suggest the possibility of synaptic interactions.

Each sensory afferent tapers somewhat as it enters the ganglion and approaches the respiratory neuropile, but the major decrease in diameter (and imputed change in transmission characteristics) seems to occur after the synaptic output region, where there is an attenuated neurite leading to the cell body.

Extracellular recordings

The records shown in Fig. 2 are representative of the extracellular responses obtained either from isolated preparations, or from suction electrodes placed on the oval organ nerve *in situ*. Not all preparations displayed three spike heights and the largest 'phasic' unit was quite frequently absent. The unit with the smallest amplitude consistently continued firing the longest.

Intracellular recordings

Systematic sampling of the large fibres in the oval organ nerve confirmed the anatomical and extracellular findings: only three fibres gave responses to pull stimuli. Penetrations of the two motor axons which run in the same nerve were easily recognized by their injury discharge upon entry, and a complete lack of responsiveness to mechanical stimulation of the oval organ.

Intracellular recordings from any of the three sensory fibres (Fig. 3) showed compound responses consisting of two distinct components, overshooting spikes and

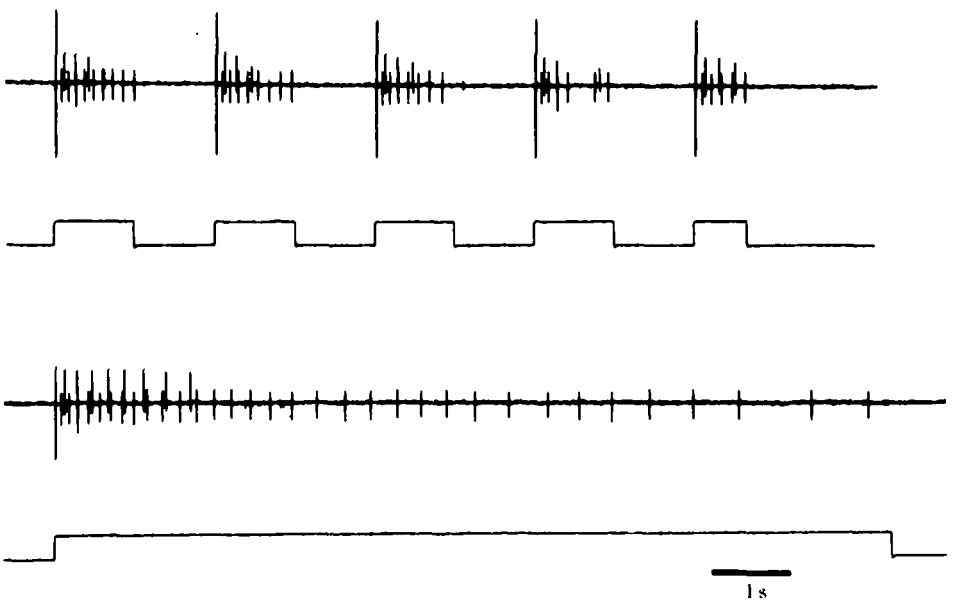

Fig. 2. Extracellular recordings from scaphognathite nerve. Responses to square wave displacements of endite sclerite (monitored on lower traces).

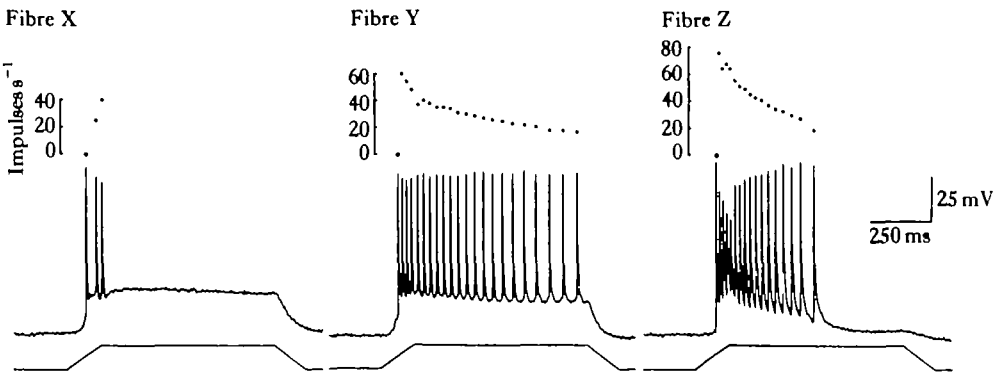

Fig. 3. Representative responses of X, Y and Z fibres to 0·8 mm pulls. Intracellular displays computer generated from taped records. Above: instantaneous frequency values obtained from reciprocals of spike intervals. Below: stimulus monitor. X and Z responses recorded concurrently; Y response taken from another, matched preparation. Electrode insertions 5·5 mm from confluence of oval organ dendrites.

graded, maintained potentials. These membrane depolarizations underlying the impulses varied in amplitude and duration with the parameter of the applied stretch, and clearly possessed the properties of receptor potentials. Normally, in afferent fibre recordings of most receptors, the receptor potential is not seen because it is a local, non-propagated event which diminishes rapidly with distance from the transducer site. Our recording electrodes were inserted 3–6 mm from the distal branch point, and yet maintained potentials up to 25 mV were not uncommon.

The two components of the sensory response, the digital spikes and the analogue receptor potentials, were not equally represented in recordings of X, Y and Z fibres as can be seen in Figs 3, 9A and 10A. In responses from the largest diameter fibre, X, the receptor potential predominated and spiking was minimal. The smallest fibre, Z, had the lowest amplitude receptor potentials during the latter part of the pull, yet the highest frequency firing during the initial period. Y fibre responses lay between these extremes. Thus from one preparation to another, each sensory fibre can easily be recognized not only by its size in relation to its neighbours, but by its physiological properties.

Effects of tetrodotoxin

Fig. 4 shows responses of a Y fibre to a series of identical trapezoidal pulls, delivered at 1-min intervals, before and after the addition of tetrodotoxin (TTX) to the preparation bath. Recordings were taken from two electrodes inserted 2·2 mm apart. 2·5 min after 8×10^{-7} M-TTX was introduced, spike amplitudes showed a noticeable decline, and spikes were completely abolished by 9·5 min leaving the receptor potentials unchanged. Thus, while the impulses depend upon fast TTX-sensitive sodium channels, the analogue signal involves other membrane channels.

It is of interest to note that in this and other similar experiments with dual electrode penetration, the spikes at the proximal locus, nearer the ganglion, declined in amplitude faster than at the distal locus, nearer the putative spike initiating zone. Both recording loci had equal access to the same concentration of TTX.

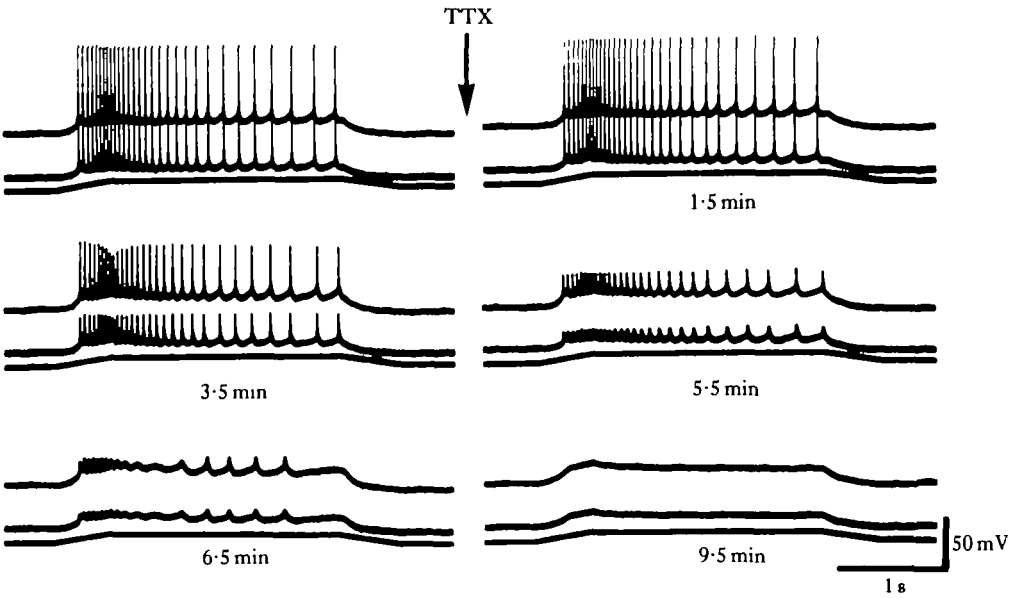

Fig. 4. Abolition of spiking from Y fibre response by 8×10^{-7} M-tetrodotoxin (TTX). Samples from a series of responses recorded at 1-min intervals. Times of exposure to TTX are indicated. Dual impalement; electrode separation 2·2 mm. Upper: distal electrode. Lower: proximal electrode.

Prolonged washing failed to reverse the blocking action of TTX, and spiking never recovered. Since the receptor potential appeared to be unaffected by TTX treatment, this gave us the opportunity to study the analogue signal in the absence of spiking and to analyse its properties.

Characteristics of the dual response

In other studies on mechanoreceptors, especially those where it has been possible to view receptor potentials directly, discrete and characteristic temporal components of the response have been recognized (Hunt & Ottoson, 1976; Bush & Roberts, 1971). With the commonly used ramp-and-hold stimulus, these components may be grouped under the headings: dynamic, static and post-release phases. In Fig. 5 a response from a TTX-treated Y fibre has been analysed according to this scheme.

Dynamic phase

At the onset of the response, the membrane depolarized rapidly, and the post-TTX responses showed a distinct point of inflection separating a steep initial component from the lesser gradient of the late dynamic component. This was reflected in a high frequency initial burst of spikes, which could be followed by a brief drop in firing rate before the spike frequency reached its dynamic peak maximum. This complex firing pattern was frequently compressed, but an example of an initial burst separated from the dynamic maximum is shown in Fig. 3(Z).

The distinction between the initial and late components of the analogue signal can be more clearly seen by comparing responses of a TTX-treated fibre to a series of

constant amplitude pulls of varying ramp velocities (Fig. 6). At the two highest velocities shown (1 mm s^{-1} and 2·5 mm s^{-1}) the entire dynamic phase had the form of an initial component, and depolarized smoothly and sharply to the dynamic peak. At lower velocities, however, the point of inflection was prominent. The late component had the same slope as the ramp of the stimulus, and reflected simply the changing length of the receptor. The dependence of the initial slope upon velocity suggests that the initial component is a function of either velocity of stretch or acceleration. Provisionally it will be referred to as the velocity response, but in a receptor of such complex geometry several explanations could be proposed and further study is warranted.

Static phase

From the dynamic peak, both graded potential and, in the case of fibres Y and Z, impulse frequency declined smoothly. As will be described more fully in the next paper (Bush & Pasztor, 1983), fibre X differs from the other two by ceasing to spike at the end of the dynamic phase and in showing very little adaptive fall in the graded potential during the static phase. Only at low amplitude pulls did the graded potential in X drop to a static plateau of lesser magnitude than the dynamic peak. Adaptation was most pronounced in fibre Z, and in some preparations the graded potential fell below the spiking threshold within 1 s (Fig. 3Z). Usually, however, the static plateau

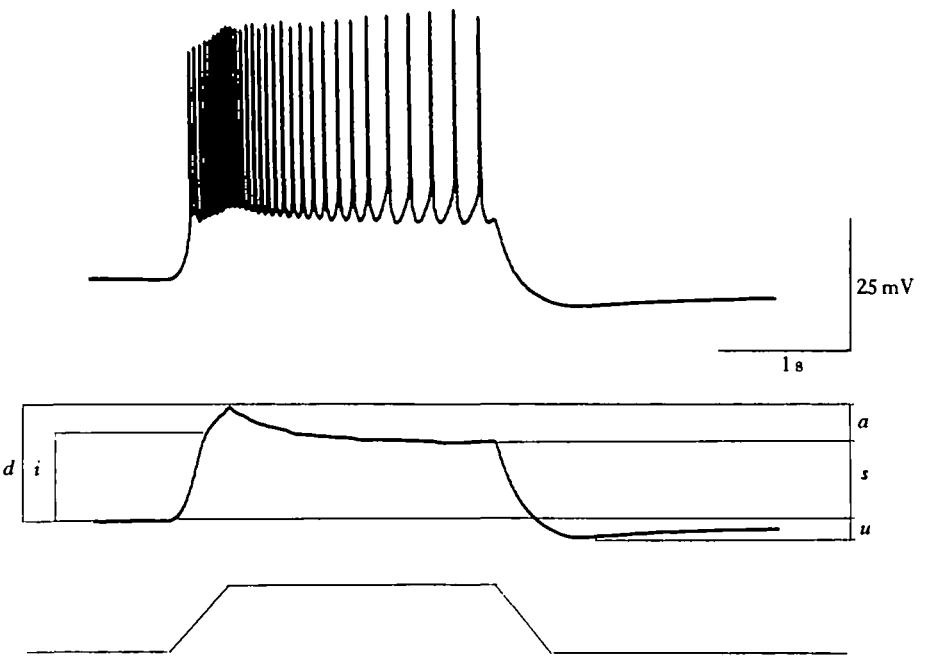

Fig. 5. Analysis of Y fibre response to trapezoidal pull before and after the application of TTX. On-line chart recordings from electrode 3 mm from confluence of sensory dendrites. Top: pre-TTX; middle: post-TTX; bottom: stimulus monitor. Pull amplitude 0·4 mm. *a*, adaptive fall; *d*, dynamic peak; *i*, initial dynamic component; *s*, static level; *u*, undershoot.

was supra-threshold and, in a series of prolonged stretches such as those shown in Fig. 7, Z fibres continued firing indefinitely, though at a lower firing rate than Y-fibres which adapt less.

Post-release phase

When the pull stimulus was terminated and the stretch was relaxed, membrane repolarization could far outlast the duration of mechanical release, and could continue into a prolonged undershoot or hyperpolarizing afterpotential. The maximum observed undershoot was 9 mV and had a duration of 40 s. This component was not observed consistently nor was its occurrence correlated with fibre type. In 37 % of all fibres tested the potential returned directly to the resting level at release with no undershoot.

The amplitude of the afterpotential depended on two factors: pull amplitude and extent of pre-stimulation stretch (or prevailing membrane potential). The two receptors represented in Fig. 7 were completely relaxed between stimuli, and, in both, the magnitude of hyperpolarization was directly correlated with pull amplitude. Duration of pull had no significant effect. Fig. 8C and D show Y and Z responses to a series of standard 0·5-mm pulls superimposed upon stepwise relaxations from a maintained stretch of 0·55 mm. In both fibres the afterpotentials were largest when the prevailing membrane potential was furthest from its true resting level. The hyperpolarizations in each case tended to restore the afferent membrane potential to that potential level associated with the fully relaxed condition.

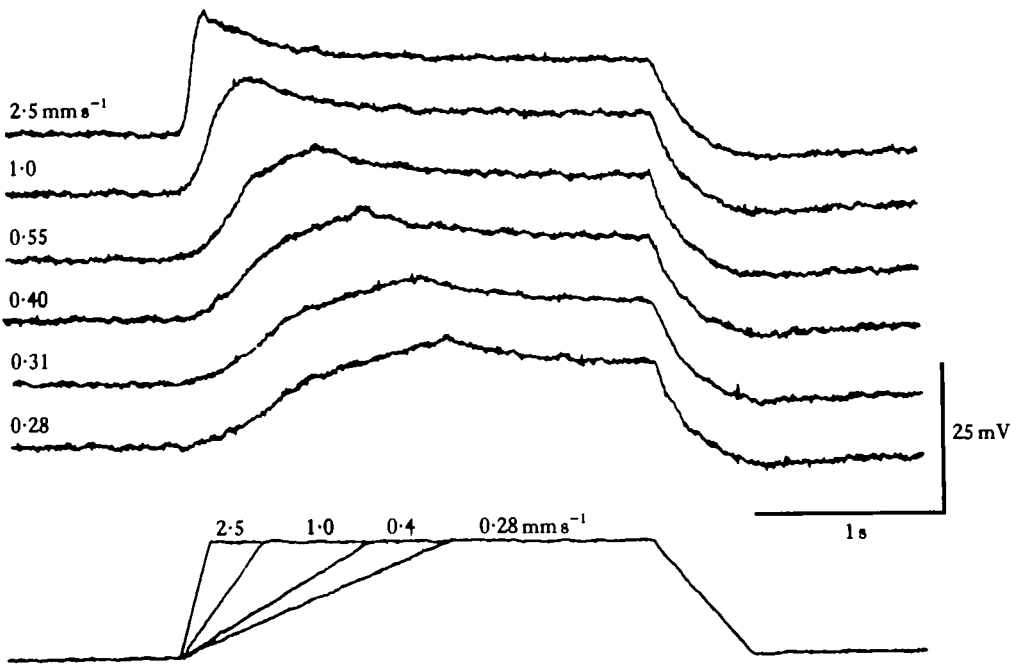

Fig. 6. Relationship between dynamic response waveform and velocity of stretch, post-TTX. Same Y fibre as in Fig. 5. (Trace irregularities due to tape noise on replay.) Pull amplitude constant at 0·4 mm; velocities as indicated.

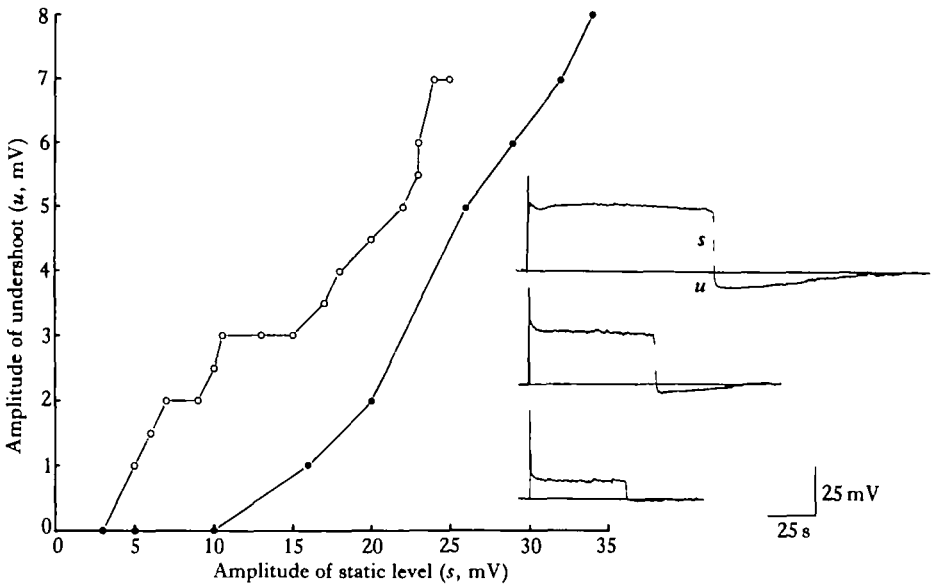

Fig. 7. Relationship between static level of membrane depolarization (s) and amplitude of hyperpolarizing undershoot (u). Open circles: values taken from X fibre responses shown in Fig. 9. 1·5-s pulls. Closed circles: values taken from another X fibre, samples shown in inset. Long pulls up to 100 s duration. Inset: horizontal line indicates the resting potential of −82 mV.

In some mechanoreceptor studies, undershoot has been shown to be correlated with previous spiking performance, and explanations based on an electrogenic sodium pump have been postulated (Nakajima & Takahashi, 1966; Sokolove & Cooke, 1971). In the oval organ, significant afterpotentials were frequently seen in the absence of spiking. Indeed, X fibres which scarcely spike, are as likely to show undershoot as the spiking fibres Y and Z (Figs 7, 8). In Fig. 8C the first pull shown produced a block in the Y fibre spiking (explained in the following paper), yet the after-hyperpolarization was of comparable size to that seen in response to the subsequent pull which produced copious spiking.

The two types of signal as information carriers

The basic stimulus parameter encoded by stretch receptors is change in length of the accessory tissue supporting the sensory dendrites. Length sensitivity in the oval organ was tested by presenting a series of constant duration pulls of increasing stretch amplitude in equal increments from 0 to 1·0 mm. Fibres were tested in pairs. Prior to the series, the initial length of the connective tissue strands was adjusted so that resting stretch was just sub-threshold for the most sensitive fibre.

Graded potentials

It has been amply demonstrated for several mechanoreceptors that the receptor potential bears a linear relationship to stretch magnitude (e.g. Katz, 1950; Eyzaguirre & Kuffler, 1955). The slope of the response curve is a measure of length sensitivity

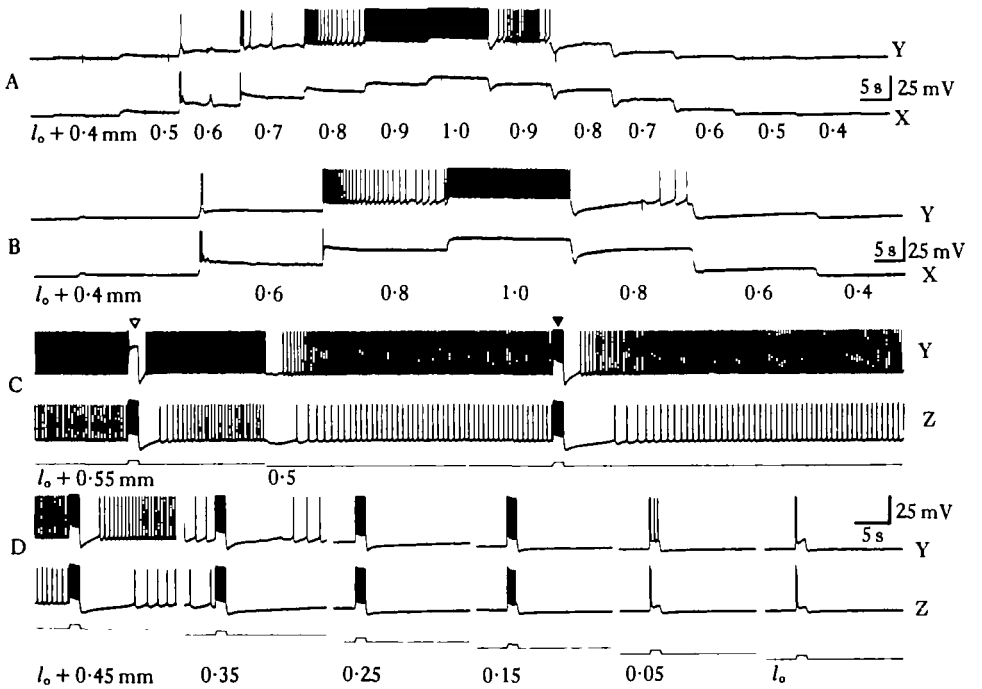

Fig. 8. Demonstrations of post-release hyperpolarizing undershoots. (A, B) Y and X responses to step stretches and relaxations. (C, D) Excerpts from a sequence of step relaxation from the stretched condition. A standard 0·5 mm pull was delivered during each level of extension. The bottom line is a monitor of both level of extension and pull. Fibres Y and Z responded with trains of continuous spiking until the length was released to 0·25 mm above rest length (l_o). Spiking was interrupted by post-release hyperpolarizations after each step relaxation and after each pull. (C) A long excerpt including two pulls (▽ and ▼) and one step relaxation. (D) Short excerpts showing responses to six uniform pulls delivered during the stages of relaxation indicated.

and the limits of the linear portion of the sigmoid curve determine the useful range over which the unit can discriminate length increments accurately. In the long oval organ afferents, considerable decrement of the receptor potential takes place, and the possibility existed that length sensitivity would be degraded and the signal would be useless as an information carrier by the time it reached the ganglion.

Fig. 9B shows a response curve for an X fibre. Static values were plotted from recordings taken 6·5 mm from the confluence of sensory dendrites; actual recordings are shown in Fig. 9A. The curve is nearly linear for pulls of 0·025–0·6 mm, after which the membrane response tends to saturate. Within this range, the sensitivity at this recording locus is 36 mV mm^{-1}. This gives an estimate of around 15 mV mm^{-1} for the signal arriving at the respiratory neuropile some 7 mm away (for $\lambda = 8$ mm: see below). Static response curves for Y and Z fibres tended to be flatter due to adaptation (see Bush & Pasztor, 1983) but their dynamic peak values gave comparable slopes. This indicates that in all three fibres, the length sensitivity of the receptor potential is preserved as the analogue signal is transmitted to the ganglion.

Spikes

Fig. 10B plots number of spikes per response against pull amplitude. The X fibre

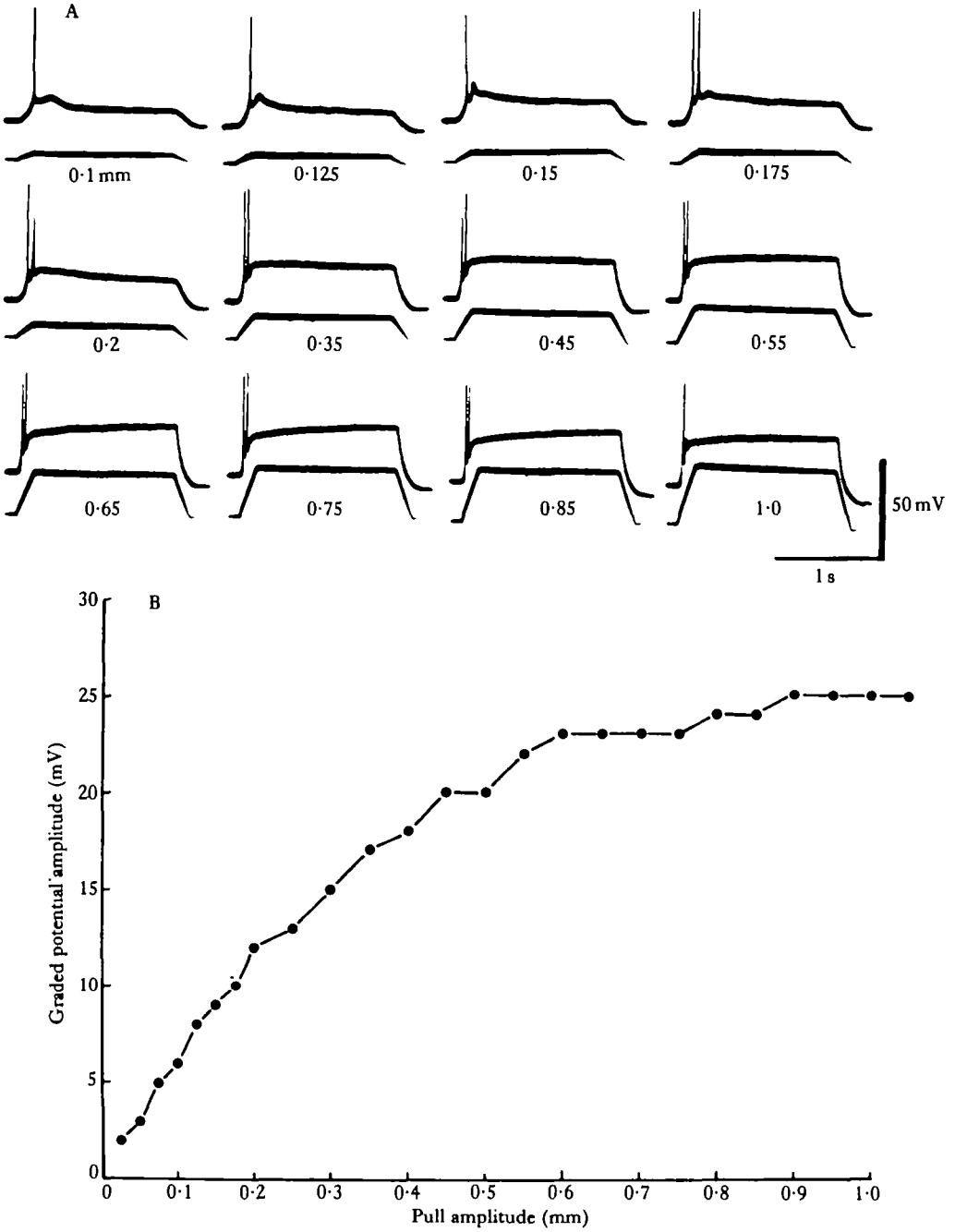

Fig. 9. Relationship between amplitude of the graded potential and amplitude of pull. (A) Responses of fibre X to a series of pulls of increasing amplitude (as indicated). (B) Fully adapted values measured at the end of the static component plotted against pull amplitude (same X series as in 9A).

in this preparation gave a maximum of two spikes per response, as did another preparation recorded in Fig. 9. Obviously the impulse signal in X is unable to encode length. But the spiking fibres Y and Z, as exemplified by Fig. 10A, have burst structures common to other spiking mechanoreceptors, and show increasing numbers

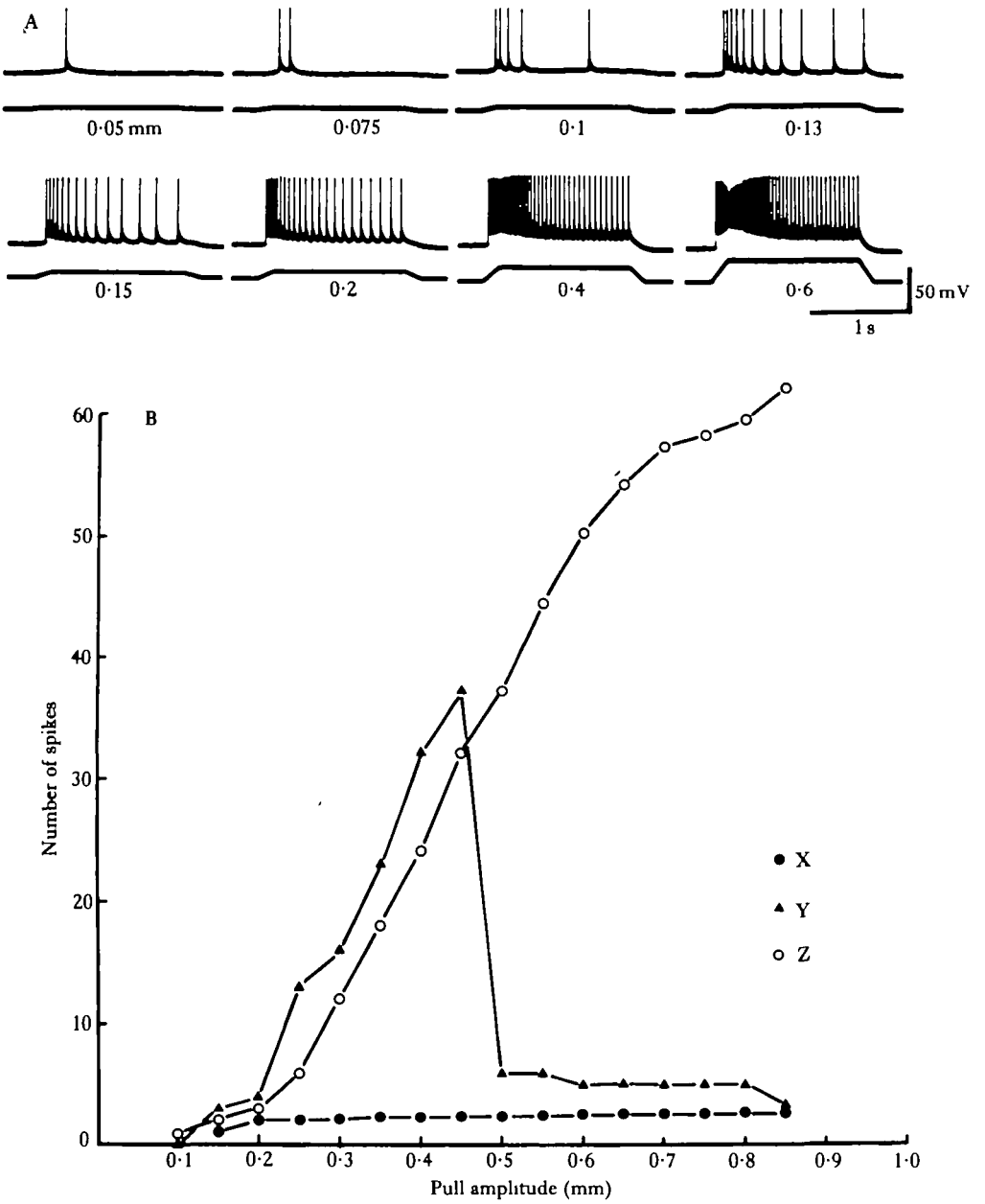

Fig. 10. Relationship between total number of spikes per response and amplitude of pull. (A) Responses of fibre Z to a series of pulls of increasing amplitude (as indicated). Duration of pull 1·5 s (including 150 ms dynamic phase). (B) Numbers of spikes per response for all three fibres X, Y and Z plotted against pull amplitude (same preparation as in 10A).

of spikes proportional to stimulus amplitude. The response curves are of similar slope over the range 0·1–0·45 mm giving a sensitivity of 130 spikes mm^{-1}. Spiking in Y inactivates at higher pull amplitudes, as described in the following paper (Bush & Rasztor, 1983).

Membrane characteristics

Length constants (λ) were calculated from steady state amplitudes of stretch-evoked receptor potentials, recorded simultaneously from two microelectrodes inserted several millimetres apart in the same fibre. Either stimulus parameters were selected so that adaptation was fully developed, giving a stable static plateau without spiking, or TTX-treated fibres were used. The mean value of λ, range (in brackets) and number of preparations of each fibre used were: X, 8·0 (6·2–9·9) mm, $N = 3$; Y, 7·2 (4·9–11·5) mm, $N = 4$; Z, 10·1 (8·7–12·0) mm, $N = 2$. At least four determinations were made on each fibre. The values ranged widely, both from one preparation to another and from one determination to another in the course of a long experiment. Membrane damage caused by the dual impalements was probably a major source of error, and it is likely that all these values are underestimates.

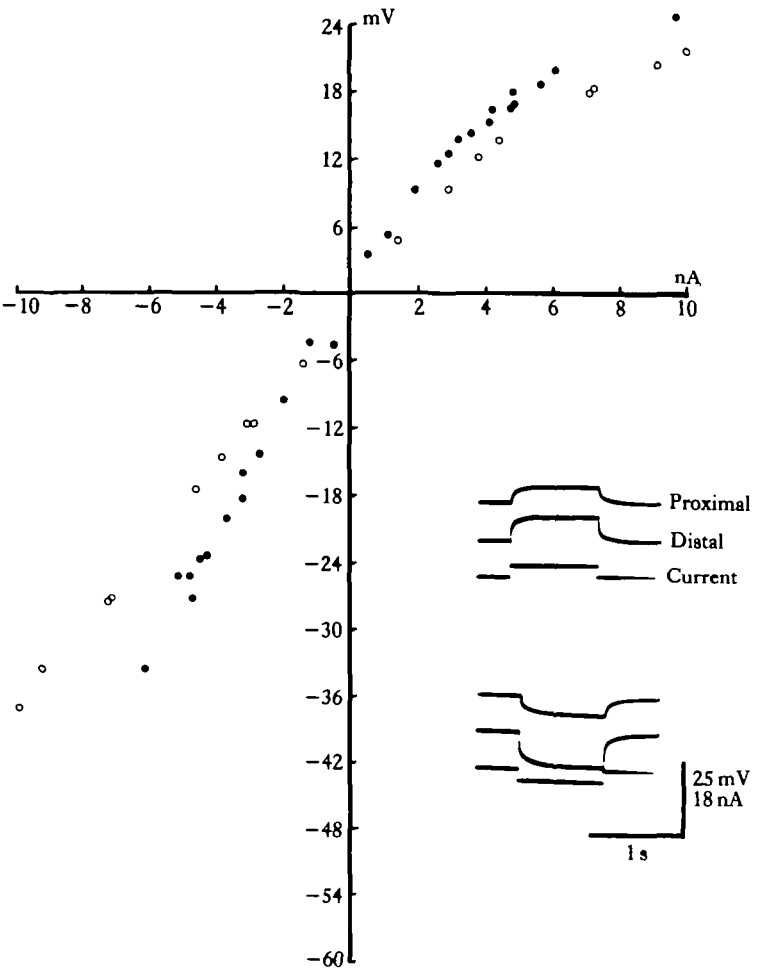

Fig. 11. Current-voltage relationship for tetrodotoxin-treated Y fibre. Dual impalement. Current injected 3 mm from oval organ (lower trace in sample record), membrane potentials recorded another 3 mm proximally (upper trace in sample record). Second series (●) recorded 45 min after first series (○).

Current-voltage curves, exemplified by Fig. 11, were obtained from TTX-treated fibres. An almost ohmic relationship is displayed over much of the voltage range, with some rectification at higher depolarizing currents. An input resistance of approximately 5 MΩ can be calculated from the slope of the linear portion (this is undoubtedly an underestimate due to decrement of the graded potential at the recording site). Specific membrane resistance (R_m) was calculated using the formula:

$$R_m = 4\lambda^2 R_i/d$$

which assumes that the afferent fibre can be represented by a cylindrical cable of semi-infinite length. Mean values of R_m for fibres X, Y and Z were 56, 58 and 167 kΩcm^2 respectively when R_i (internal axoplasmic resistance) was given the same 90 kΩcm value used by Shaw (1972). These values compare favourably with his estimates for the non-spiking barnacle photoreceptor afferents.

DISCUSSION

Three examples of mechanoreceptors with central cell bodies and thick afferent fibres have been documented: the T-C MRO at the base of decapod Crustacean walking legs (Ripley *et al.* 1968; Bush, 1981), the giant neurones in the uropods of the anomuran sand crab *Emerita* (Paul, 1972) and the NSSRs at the base of the swimmerets in crayfish (Heitler, 1982). To this group must now be added the oval organ at the base of the second maxilla in lobster, rock lobster and crab. They all share membrane properties which minimize the normal attenuation of local graded potentials, so that stretch-induced depolarizations of the terminals are conducted along afferent fibres to the ganglion. Where oval organ afferents differ dramatically is that they can also initiate and support regenerative impulses, whereas the other three examples cannot.

Both the S and T fibres of the T-C MRO occasionally display small spike-like potentials which are blocked by TTX (Roberts & Bush, 1971). They are, however, graded, non-regenerative, their occurrence is sporadic and their function is uncertain. By contrast, the spikes of X, Y and Z oval organ fibres are true overshooting, regenerative impulses which consistently form part of the sensory response, and whose firing frequencies correlate predictably with stimulus parameters. Both Y and Z fibres have a range of firing frequency, and sensitivity to small stimulus increments, which compare favourably, for example, with that of the abdominal MRO.

Characteristics of the graded potentials

The graded potentials of the oval organ afferents have waveforms resembling those of the S fibres of the T-C MRO (Bush & Roberts, 1971) and the NSSRs of the crayfish swimmeret (Heitler, 1982). The major contribution derives from a direct dependence of membrane potential upon receptor length, and velocity-dependent components are of lesser importance. The prominent dynamic response of the T fibre, with its pronounced velocity sensitivity, finds no parallel in the X, Y or Z responses. This lack, correlated with the absence of muscle tissue from the oval organ structure, lends support to the hypothesis that dynamic sensitivity is in large measure a consequence of an association between sensory fibre terminals and a viscoelastic element such as

a receptor muscle. In the oval organ (Pasztor, 1979), the zone between the epidermis (which provides anchorage for the sensory terminals) and the collagenous connective tissue strands (which support the secondary dendrites) has a matrix of the same amorphous connective tissue that surrounds both the crab S fibre terminals (Whitear, 1965; Krauhs & Mirolli, 1975) and the terminals of the slowly adapting unit of the crayfish abdominal MRO (Euteneuer & Winter, 1979; Komuro, 1981). As in these other receptors, it is probably a region of elastic compliance and, similarly, may be the site of mechano-electric transduction.

The amplitudes of oval organ and S fibre depolarizations fall within similar ranges in response to similar stretches. Recordings of 10–20 mV for elongations of 0·5 mm are common in both receptors (Bush & Roberts, 1971, and the current study). These values, however, were recorded several millimetres from the distal branch point, and actual values near the transducer region are likely to be of the order of 20–40 mV. These are somewhat larger depolarizations than have been seen in other impulse-signalling mechanoreceptors which have been studied intracellularly, for example 10–25 mV for generator potentials recorded from the cell bodies of crustacean abdominal MROs (Nakajima & Onodera, 1969). No doubt the larger responses are advantageous for receptors which make use of decremental graded potentials for signalling.

Central efficacy of graded signalling

It has been well established that non-impulsive S and T fibre responses not only reach the neuropile, but can initiate and modulate motoneurone firing (Bush, 1977, 1981; Blight & Llinas, 1980; Cannone & Bush, 1980, 1981, 1982). Similarly, Paul (1972) and Heitler (1982) have shown that current injection into the non-spiking stretch receptor neurones can excite or inhibit motoneurones of the sand crab uropods and crayfish swimmerets respectively. Our values for the length constant (λ = about 1 cm) approximate the total distance which the analogue signal must travel from the confluence of the sensory dendrites to the synaptic region within the neuropile. Thus the graded potentials could diminish by some 63 % before they reach the site of transmitter release, and would represent much smaller depolarizations than the 35 mV maxima recorded in the swimmeret neuropile (Heitler, 1982). However, our estimates of λ are undoubtedly underestimates (see discussion by Bush, 1981, on length constant values measured by Mirolli, 1979). Even with a 63 % decrement, most of the range of potentials recorded from our mid-length impalements could theoretically release significant amounts of transmitter at the central terminals. Indeed Schmitt, Dev & Smith (1976) postulated that transmitter release could be triggered by membrane potentials of just a few tenths of a millivolt. Burrows (1979) found that presynaptic depolarizations of 2 mV were sufficient to effect chemical transmission between an insect non-spiking premotor interneurone and a motoneurone. Furthermore, Blight & Llinas (1980) demonstrated conclusively that small changes in presynaptic voltage could be effective in producing postsynaptic potentials in the crab T-C MRO stretch reflex.

Other examples of dual signalling

Having presented evidence that two types of signal, the analogue graded potential and the frequency coded impulses are available for information transfer, we must ask

the question: does the nervous system actually utilize both signals? Several studies suggest that neural circuits do exist capable of responding to both types of signal. Burrows (1980) and Burrows & Siegler (1982) found two populations of local premotor interneurones in insect ganglia, one spiking and the other non-spiking. They have similar anatomy and both types appear to play well defined roles in modulating motoneurone activity, suggesting that either mode of transmission is equally effective. Dickinson, Nagy & Moulins (1981) demonstrated functional spiking and non-spiking transmission in different branches of individual lobster stomatogastric neurones. Dual signalling is quite common in visual interneurones, notably amacrine cells in vertebrate retinas and L-neurones in insect ocelli. Milde (1981) showed that honey bee L-neurones can function in either the spiking or the non-spiking mode, and he postulated that there might be selective synaptic mechanisms specific for graded potentials or spikes. He presented behavioural evidence supporting the notion that both signals are utilized. Simmons (1982) identified excitatory connections between L-neurones in locusts which can transmit without spikes and inhibitory ones where spikes are required.

Evidence for dual signalling in primary afferents is sparse and limited to molluscan photoreceptors (reviewed by Chase, 1975). Alkon (1973) showed that short afferents (120 μm in length) conducted both graded potentials and spikes into the ganglion, but in his published figures only spikes are correlated with postsynaptic events.

Possible significance of dual signalling in the oval organ

Two aspects of the respiratory system in decapod Crustacea encourage our belief that the graded potentials transmitted along X, Y and Z fibres are information carrying signals which supplement, to a significant degree, the more usual impulse-coded system. The first is the nature of the activity the oval organ must monitor. During gill ventilation, the second maxilla is performing a cyclical beat at frequencies of 50–120 min^{-1}. This implies that the length changes within the receptor are approximately sinusoidal, and stretches evoking responses above the firing threshold may be limited to only a short duration. But in the branchial pump both strokes of the scaphognathite, namely elevation and depression, are significant components of the water pumping cycle, and it would be advantageous to have continuous monitoring of the whole cycle. The discontinuous brief bursts of impulses at the peak stretches, from such a small population of afferents, could not code all the parameters important as feedback for the scaphognathite motor programme. On the other hand, the analogue signal is a continuous source of information, and depolarizes and hyperpolarizes in phase with the sinusoidal stimulus. The hyperpolarizing undershoot, which is augmented by a sudden relaxation, could provide information about change in portions of the cycle ignored by the spiking mechanism.

Secondly, the demonstration of non-impulsive transmission within the respiratory pattern generating system of Crustacea (Simmers & Bush, 1980, 1983) makes it likely that key elements in the oscillator network are well adapted to responding to small increments or decrements in transmitter released by graded presynaptic events.

Bullock (1981) has speculated that we should expect to find both graded and impulsive transmission throughout the central nervous system. The oval organ may provide a useful model for studying dual signalling within single neurones.

This work was supported by research grants to BMHB from the Royal Society and the Science Research Council (U.K.) and to VMP from the Natural Sciences and Engineering Research Council of Canada. We thank Alison Walford for technical assistance.

REFERENCES

ALEXANDROWICZ, J. S. & WHITEAR, M. (1957). Receptor elements in the coxal region of Decapoda Crustacea. *J. mar. biol. Ass. U.K.* **36**, 603–628.

ALKON, D. L. (1973). Neural organization of a molluscan visual system. *J. gen. Physiol.* **61**, 444–461.

BACON, J. P. & ALTMAN, J. S. (1977). A silver intensification method for cobalt-filled neurones in wholemount preparations. *Brain Res.* **138**, 359–363.

BLIGHT, A. R. & LLINÁS, R. (1980). The non-impulsive stretch-receptor complex of the crab: a study of depolarization-release coupling at a tonic sensorimotor synapse. *Phil. Trans. R. Soc. Ser. B* **290**, 219–276.

BULLOCK, T. H. (1981). Spikeless neurones: where do we go from here? In *Neurones without Impulses*, (eds A. Roberts & B. M. H. Bush), pp. 269–284. Cambridge: Cambridge University Press.

BURROWS, M. (1979). Synaptic potentials effect the release of transmitter from locust non-spiking interneurons. *Science, N.Y.* **204**, 81–83.

BURROWS, M. (1980). The control of sets of motoneurones by local interneurones in the locust. *J. Physiol., Lond.* **298**, 213–233.

BURROWS, M. & SIEGLER, M. B. S. (1982). Spiking local interneurones mediate local reflexes. *Science, N.Y.* **217**, 650–652.

BUSH, B. M. H. (1976). Non-impulsive thoracic-coxal receptors in crustaceans. In *Structure and Function of Proprioceptors in the Invertebrates*, (ed. P. J. Mill), pp. 115–151. London: Chapman & Hall.

BUSH, B. M. H. (1977). Non-impulsive afferent coding and stretch reflexes in crabs. In *Identified Neurons and Behaviour of Arthropods*, (ed. G. Hoyle), pp. 439–460. New York: Plenum.

BUSH, B. M. H. (1981). Non-impulsive stretch receptors in crustaceans. In *Neurones without Impulses*, (eds A. Roberts & B. M. H. Bush), pp. 147–176. Cambridge: Cambridge University Press.

BUSH, B. M. H., GODDEN, D. H. & MACDONALD, G. A. (1975). A simple and inexpensive servo system for the control of length or tension of small muscles or stretch receptors. *J. Physiol., Lond.* **254**, 1–3.

BUSH, B. M. H. & LAVERACK, M. S. (1982). Mechanoreception. In *Neurobiology: Structure and Function*, (eds H. L. Atwood & D. C. Sandeman), pp. 399–468, Vol. 3 of *The Biology of Crustacea*, (ed. D. E. Bliss). New York & London: Academic Press.

BUSH, B. M. H. & PASZTOR, V. M. (1983). Graded potentials and spiking in single units of the oval organ, a mechanoreceptor in the lobster ventilatory system. II. Individuality of the three afferent fibres. *J. exp. Biol.* **107**, 451–464.

BUSH, B. M. H. & ROBERTS, A. (1971). Coxal muscle receptors in the crab: the receptor potential of S and T fibres in response to ramp stretches. *J. exp. Biol.* **55**, 813–832.

CANNONE, A. J. & BUSH, B. M. H. (1980). Reflexes mediated by non-impulsive afferent neurones of thoracic-coxal muscle receptor organs in the crab, *Carcinus maenas*. I. Receptor potentials and promotor motoneurone responses. *J. exp. Biol.* **86**, 275–303.

CANNONE, A. J. & BUSH, B. M. H. (1981). Reflexes mediated by non-impulsive afferent neurones of thoracic-coxal muscle receptor organs in the crab, *Carcinus maenas*. III. Positive feedback to the receptor muscle. *J. comp. Physiol.* **142**, 103–112.

CANNONE, A. J. & BUSH, B. M. H. (1982). Dual reflex motor control of non-spiking crab muscle receptor. I. Positive feedback tonically reduced and dynamically stabilized by concurrent inhibition of Rm1. *J. comp. Physiol.* **148**, 365–377.

CHASE, R. (1975). The electrophysiology of transduction, retinal interaction and axonal conduction in invertebrate photoreceptors. *Comp. Biochem. Physiol.* **52**A, 571–576.

DICKINSON, P. S., NAGY, F. & MOULINS, M. (1981). Interganglionic communication by spiking and nonspiking fibers in the same neuron. *J. Neurophysiol.* **45**, 1125–1138.

EUTENEUER, U. & WINTER, C. (1979). The abdominal muscle receptor organ in *Astacus leptodactylus* (Crustacea). A fine structural analysis. *Cell Tiss. Res.* **202**, 41–61.

EYZAGUIRRE, C. & KUFFLER, S. W. (1955). Processes of excitation in the dendrites and in the soma of single isolated sensory nerve cells of the lobster and crayfish. *J. gen. Physiol.* **39**, 87–119.

HEITLER, W. J. (1982). Non-spiking stretch-receptors in the crayfish swimmeret system. *J. exp. Biol.* **96**, 355–366.

HUNT, C. C. & OTTOSON, D. (1976). Initial burst of primary endings of isolated mammalian muscle spindles. *J. Neurophysiol.* **39**, 324–330.

KATZ, B. (1950). Depolarization of sensory terminals and the initiation of impulses in the muscle spindle. *J. Physiol., Lond.* **111**, 261–282.

KOMURO, T. (1981). Fine structural study of the abdominal muscle receptor organs of the crayfish (*Procambarus clarkii*). Sensory endings and synaptic structures. *J. Neurocytol.* **10**, 27–43.

KRAUHS, J. M. & MIROLLI, M. (1975). Morphological changes associated with stretch in a mechano-receptor. *J. Neurocytol.* **4**, 231–246.

MILDE, J. (1981). Graded potentials and action potentials in the large ocellar interneurons of the Bee. *J. comp. Physiol.* **143**, 427–434.

MIROLLI, M. (1979). The electrical properties of a crustacean sensory dendrite. *J. exp. Biol.* **78**, 1–27.

NAKAJIMA, S. & ONODERA, K. (1969). Adaptation of the generator potential in the crayfish stretch receptors under constant length and constant tension. *J. Physiol., Lond.* **200**, 187–204.

NAKAJIMA, S. & TAKAHASHI, K. (1966). Post-tetanic hyperpolarization and electrogenic Na-pump in stretch receptor neurone of crayfish. *J. Physiol., Lond.* **187**, 105–127.

PASZTOR, V. M. (1969). The neurophysiology of respiration in decapod crustacea. II. The sensory system. *Can. J. Zool.* **47**, 435–441.

PASZTOR, V. M. (1979). The ultrastructure of the oval organ, a mechanoreceptor in the second maxilla of decapod crustacea. *Zoomorphologie* **193**, 171–191.

PASZTOR, V. M. & BUSH, B. M. H. (1982). Impulse-coded and analog signaling in single mechanoreceptor neurons. *Science, N.Y.* **215**, 1635–1637.

PAUL, D. H. (1972). Decremental conduction over 'giant' afferent processes in an arthropod. *Science, N.Y.* **176**, 680–682.

RIPLEY, S. H., BUSH, B. M. H. & ROBERTS, A. (1968). Crab muscle receptor which responds without impulses. *Nature, Lond.* **218**, 1170–1171.

ROBERTS, A. & BUSH, B. M. H. (1971). Coxal muscle receptors in the crab: the receptor current and some properties of the receptor nerve fibres. *J. exp. Biol.* **54**, 515–524.

SCHMITT, F. O., DEV, P. & SMITH, B. H. (1976). Electrotonic processing of information by brain cells. *Science, N.Y.* **193**, 114–120.

SHAW, S. R. (1972). Decremental conduction of the visual signal in the barnacle lateral eye. *J. Physiol., Lond.* **220**, 145–175.

SIMMERS, A. J. & BUSH, B. M. H. (1980). Non-spiking neurones controlling ventilation in crabs. *Brain Res.* **197**, 247–252.

SIMMERS, A. J. & BUSH, B. M. H. (1983). Central nervous mechanisms controlling rhythmic burst generation in the ventilatory motoneurones of *Carcinus maenas*. *J. comp. Physiol.* **150**, 1–21.

SIMMONS, P. J. (1982). Transmission mediated with and without spikes at connexions between large second-order neurones of locust ocelli. *J. comp. Physiol.* **147**, 401–414.

SOKOLOVE, P. G. & COOKE, I. M. (1971). Inhibition of impulse activity in a sensory neuron by an electrogenic pump. *J. gen. Physiol.* **57**, 125–163.

WHITEAR, M. (1965). The fine structure of crustacean proprioreceptors. II. The thoracico-coxal organs in *Carcinus, Pagurus* and *Astacus*. *Phil. Trans. R. Soc. Ser. B* **248**, 437–456.